Study of the macro-scale transition emerging from non-Newtonian fluid flow through porous media

Frédéric Zami-Pierre, Yohan Davit, Romain De Loubens, Michel Quintard

Study of the macro-scale transition emerging from non-Newtonian fluid flow through porous media

F. Zami-Pierre* (Total), Y. Davit (CNRS), R. de Loubens (Total) & M. Quintard (CNRS)

SUMMARY

Over the last decades, the intensive use of polymer mixtures in Enhanced Oil Recovery (EOR) has led to a great effort in understanding the flow of such fluids through complex porous media. While the macro-scale behavior of these fluids has been actively investigated using core-scale experiments, the link with the micro-scale fundamental physics of the flow remains largely unexplored. A transition from a Newtonian to a non-Newtonian macro-scale regime has been observed. Recently, a simple model has been proposed to characterize the critical Darcy velocity associated to this transition phenomenon. Here, we use computational fluid dynamics, conceptual porous media and experimental datasets provided by the literature to test the robustness this model. We conclude that the model is valid. Furthermore, it allows, via an explicit formulation, a better understanding of the critical Darcy velocity associated to the transition.

Introduction

The flow of non-Newtonian fluids through porous media is ubiquitous in many applications, such as blood flow [1], polymer flows in composites and paper manufacturing [2] or enhanced oil recovery [3-5]. Understanding the underlying physics and proposing models for such complex flows is both intriguing and fundamental. Polymer solutions – typically Xanthan or Dextran in water – are classical examples of non-Newtonian fluids. Flow of such polymer solutions through porous media has been the subject of intense experimental and modeling works. Difficulties for all of these studies lie in the multiscale nature of porous media and highly nonlinear nature of the fluids rheology.

For Newtonian fluids, Darcy's law is a remarkable example of a simple and robust homogenized expression where the system is described using the filtration velocity $\langle U \rangle$ and the macro-scale pressure gradient ∇p,

$$\langle \boldsymbol{U} \rangle = -\frac{\boldsymbol{K} \cdot \nabla P}{\mu}. \tag{1}$$

In Eq. 1, $\boldsymbol{K}$ is the permeability tensor, μ is the viscosity of the fluid and $\nabla P = \nabla p - \rho \boldsymbol{g}$ the hydrodynamic pressure gradient. Due to the complex pore structure, the pore-scale flow field exhibits large perturbations from spatially average fields. These perturbations are further coupled with the strong nonlinear effects induced by the presence of the polymers, e.g., shear thickening and thinning, yield stress and cut-off effects, time-dependent mechanisms, mechanical and chemical degradation of polymer chains, confinement and sorption effects. The variety of phenomena occurring at the pore-scale, and even at smaller scales, is actually very large. Under these circumstances, devising accurate models that apply to the Darcy or reservoir scales is an important challenge.

Although the physics of non-Newtonian fluids represents a wide domain, many polymer mixtures exhibit similar rheological features. Under low shear rate, the fluid can often be considered Newtonian – i.e., with a uniformly constant viscosity μ_0 – while under high shear rate, a power-law behavior is observed, $\mu \propto \dot{\gamma}^{n-1}$ with $\dot{\gamma}$ the local shear rate and n an intrinsic exponent of the fluid. The flow of such fluids through a porous medium yields two different macro-scale behaviors (Newtonian and non-Newtonian). During the past decades, thorough studies have been performed to understand and predict the transition between the two resulting macro-scale laws. The complexity of this problem lies in both the nonlinearity induced by the fluid rheology and the complex pore structure of the medium itself. Recently, a simple prediction of the critical condition at which the macro-scale behavior transitions from Newtonian to non-Newtonian has been proposed by Zami-Pierre et al [6]. This model predicts a critical average velocity characterizing the regime at which the apparent homogenized behavior starts to become nonlinear.

The goal of this paper is to provide more insight into the analysis previously proposed in [6], using simple analytical solutions over bundles of tubes and experimental datasets provided by the literature. This paper is organized as follows. After a review of previous work, we present the rheological model used. Then, we compare the critical velocity model to analytical solutions obtained for tube bundles. Later, we compare the model to experimental datasets. Finally, we investigate the relative invariance of the flow patterns when increasing velocity, for the porous media used in the previous study by Zami-Pierre et al [6].

Previous work

As described in the introduction, the flow of non-Newtonian fluids through porous media has been the subject of intensive work. In this paper, we focus on relatively simple non-Newtonian fluids. We consider a constitutive law whereby the viscosity is constant up to a critical shear rate $\dot{\gamma}_c$, and then follows a classical power law. This behavior has been observed for many polymer mixtures using standard measurements techniques. At the macro-scale, Newtonian – constant permeability – and non-

Newtonian – variable permeability – regimes are observed. As demonstrated theoretically [7-9], experimentally [10,11] and computationally [12,13], the non-Newtonian permeability for power-law fluids evolves as $\propto \|\langle U\rangle_{FL}\|^{1-n}$, $\langle U\rangle_{FL}$ being the intrinsic average velocity in the porous medium.

A common method used in core-flood experiments to evaluate the constraints experienced by the fluid inside the porous medium consists in calculating an apparent shear rate as $\dot{\gamma}_{app} = 4\alpha\langle U\rangle / R_{app}$, [14-16]. This formulation is directly deduced from a single tube analogy, where the length R_{app} is proportional to the square root of the Newtonian permeability. At the transition, we should have $\dot{\gamma}_{app} = \dot{\gamma}_c$ for a real porous medium. However, a semi-empirical parameter α is necessary to calibrate the actual transition. It is not surprising that a single tube analogy is not sufficient to understand the complexity due to the porous structure and the fluid rheology. Moreover, many other physical phenomena may be involved in the fitting parameter α such as slip, sorption, etc.

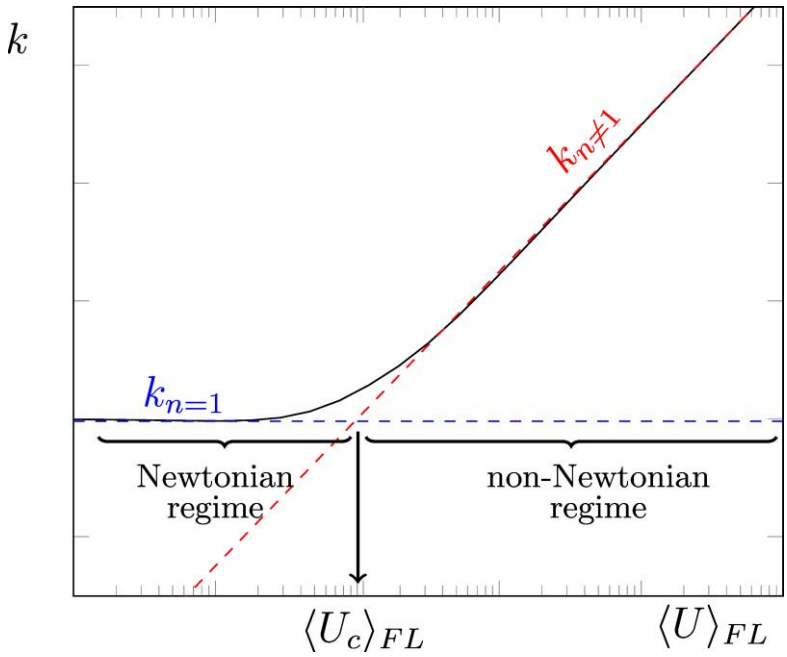

Figure 1 *Evolution of the apparent permeability versus the intrinsic average velocity. This behavior is valid for any porous medium while a relatively simple non-Newtonian fluid – here Newtonian at low shear rates and then shear-thinning – is flowing through it. We observe two distinct macro-scale regimes. The Newtonian permeability corresponds to* $k_{n=1}$ *and the non-Newtonian asymptote to* $k_{n\neq1}$.

More recently, a new approach to quantify the transition has been proposed in [6] based on direct numerical simulations of the flow field over a wide panel of different porous media, e.g., model porous media such as simple arrays, beads packing or tomographic images of sandstone samples. An important finding is that the macroscopic transition to a non-Newtonian regime is controlled by the local transition in a limited number of pore-throats. From a dimensional analysis and the study of viscous dissipation, we found a model that characterizes the transition using only an effective length scale. This yields a new formulation for the intrinsic average velocity at which the macro-scale behavior transitions, which reads

$$\langle U_c\rangle_{FL} = \dot{\gamma}_c\sqrt{k_{n=1}}, \tag{2}$$

with $k_{n=1}$ the Newtonian permeability. This model is found to predict the transition with relatively good accuracy. An important feature here is the absence of any fitting parameter and the prediction of the transition using a simple effective length that is based on the linear situation. The goal of the

present paper is to propose a test of robustness for the model presented in Eq. 2. The approach consists in comparing this model to tube bundles to see if the underlying theory remains valid.
Rheological model

The fluid's rheology is chosen as time independent and viscosity is a simple function of the local shear rate. The chosen rheological model is a power law with cut-off (PLCO), like in [6]. This model uses two parameters, (n and $\dot{\gamma}_c$) as described in Eq. 3 below,

$$\mu = \begin{cases} \mu_0 & if\ \dot{\gamma} < \dot{\gamma}_c, \\ \mu_0 \left(\frac{\dot{\gamma}}{\dot{\gamma}_c}\right)^{n-1} & otherwise. \end{cases} \quad (3)$$

In Eq. 3, the local shear rate is defined as $\dot{\gamma} = \sqrt{\frac{1}{2}(\nabla U + \nabla U^t) : (\nabla U + \nabla U^t)}$. The parameter n indicates the rheological response of the fluid with the shear rate. A Newtonian fluid corresponds to $n = 1$ – which is the reason why the Newtonian permeability is denoted by $k_{n=1}$ in this paper – whereas shear-thinning corresponds to $n < 1$ and shear-thickening to $n > 1$. The higher $|n - 1|$, the stronger is the nonlinearity induced by the fluid. This model is known to accurately describe many polymer solutions. The parameters n and $\dot{\gamma}_c$ can be obtained by standard rheological measurements. Due to the relative simplicity of this model, analytical solutions can be obtained for simple geometries, as shown in the following section.

Model comparison with tubes bundles

Analytical tubes bundles have been intensively studied in porous media science [17]. More specifically, for purely non-Newtonian fluids, the analogy with tubes bundles has already been used to explain the macro-scale behavior observed experimentally [18-19]. On the other hand, the transition phenomenon between Newtonian and non-Newtonian macro-scale regimes has surprisingly not been studied using bundles of tubes and analytical solutions.

Figure 1 shows the apparent permeability of a PLCO fluid flowing through a porous medium. We observe two macro-scale regimes, with a Newtonian and a non-Newtonian asymptote. The critical velocity $\langle U_c \rangle_{FL}$ is defined as in [6] as the intersection of the fully non-Newtonian asymptote with the Newtonian permeability line, see Fig. 1. Here we investigate the behavior of $\langle U_c \rangle_{FL}$ for porous media consisting of a single tube, bundles of tubes in serial and in parallel. For all these media, we have calculated the Newtonian ($\mu = \mu_0$) permeability $k_{n=1}$ and the apparent non-Newtonian ($\mu \propto \dot{\gamma}^{n-1}$) permeability $k_{n\neq1}$. We then calculate the critical velocity $\langle U_c \rangle_{FL}$ defined as the average velocity $\langle U \rangle_{FL}$ at which $k_{n=1} = k_{n\neq1}$. Finally, we express this critical velocity with an effective length, ℓ_{eff}, and the rheological parameter $\dot{\gamma}_c$ as $\langle U_c \rangle_{FL} = \dot{\gamma}_c \ell_{eff}$. The bundles of tubes are composed of N tubes of radii R_i ($1 \leq i \leq N$). For the specific case of the serial bundle, each tube i has an associated length h_i. For the case of the parallel bundle, all tubes have the same length h_0. All our calculations are summarized in Table 1.

In Table 1, the factor $C(n)$ might be different from values found in the literature, like for instance in [4,20]. This may be explained by a different definition of the transition point, emerging from a single tube. Here we used the asymptote intersection method defined above (see Fig. 1), while others would use the velocity at which the maximum shear rate in the medium is equal to the critical shear rate $\dot{\gamma}_c$. This latter definition emphasizes the departure from the pure Newtonian flow and the beginning of the complex transition regime. Our proposed definition offers a better mathematical connection between the two limited regimes.

	Single tube	Tubes in serial	Tubes in parallel
$k_{n=1}$	$\frac{R^2}{8}$	$\frac{\sum_i h_i}{R_{eq}^2 \sum_i \frac{8h_i}{R_i^4}}$	$\frac{1}{8}\frac{\sum_i R_i^4}{\sum_i R_i^2}$
$k_{n\neq1}$	$A(n,\dot{\gamma}_c)\, R^{n+1} \langle U \rangle_{FL}{}^{1-n}$	$A(n,\dot{\gamma}_c)\, \frac{\sum_i h_i}{R_{eq}^{2n} \sum_i \frac{h_i}{R_i^{3n+1}}} \langle U \rangle_{FL}{}^{1-n}$	$A(n,\dot{\gamma}_c) \left(\frac{\sum_i R_i^{3+1/n}}{\sum_i R_i^2}\right)^n \langle U \rangle_{FL}{}^{1-n}$
ℓ_{eff}	$R\ C(n)$	$\left(\frac{R_{eq}^{2n} \sum_i \frac{h_i}{R_i^{3n+1}}}{R_{eq}^2 \sum_i \frac{8h_i}{R_i^4}}\right)^{\frac{1}{1-n}} C(n)$	$\left(\frac{\sum_i R_i^4}{\sum_i R_i^2}\left(\frac{\sum_i R_i^2}{\sum_i R_i^{3+1/n}}\right)^n\right)^{\frac{1}{1-n}} C(n)$

Table 1 *Calculated Newtonian and non-Newtonian permeability and related effective length used in* $\langle U_c \rangle_{FL}$ *to characterize the macro-scale transition. In this table, the following definitions are used:* $A(n,\dot{\gamma}_c) = \left(\frac{n}{3n+1}\right)^n \frac{\dot{\gamma}_c{}^{n-1}}{2}$, $C(n) = \left(\frac{1}{4}\left(\frac{3n+1}{n}\right)^n\right)^{\frac{1}{1-n}}$ *and* $R_{eq}^2 = \frac{\sum_i h_i R_i^2}{\sum_i h_i}$.

We remark that, for the bundles of tubes in parallel or in serial, we naturally recover the single tube case by reducing the number of tubes to one. We also remark that the parameter $C(n)$ comes as a factor for the effective length in all cases. For strong variations of n, $0.5 < n < 1.5$, this factor verifies the double inequality $0.88 < 2\sqrt{2}\mathrm{C}(n) < 0.91$. Hence, we approximate it by $1/2\sqrt{2}$ (approximation valid to about 4%). As a consequence, we obtain in the single tube case $\ell_{eff} = R \times C(n) \simeq \frac{R}{2\sqrt{2}} = \sqrt{k_{n=1}}$, which is coherent with the findings in Zami-Pierre et al. (2016). For the other porous media, the results are less clear and actual computations of ℓ_{eff} over discrete distributions are needed.

We adopt a discrete log-normal distribution for *N* tubes. For the sake of simplicity and to reduce the number of variables, all tubes have the same length h_0 in the case of a serial bundle. We use a large number of tubes (10^7), in order to have representative statistics. The distribution is defined by a mean value of radii R_{mean} and a variance v. In addition, we calculate for each parallel or serial bundle the effective length associated to the macro-scale transition ℓ_{eff} and the Newtonian permeability $k_{n=1}$ of the generated porous medium. We plot, Fig. 2, the dimensionless effective length $\ell_{eff}^* = \ell_{eff}/\sqrt{k_{n=1}}$ against the variance of these porous media. We added the value ℓ_{eff}^* for the porous media investigated in the previous study [6].

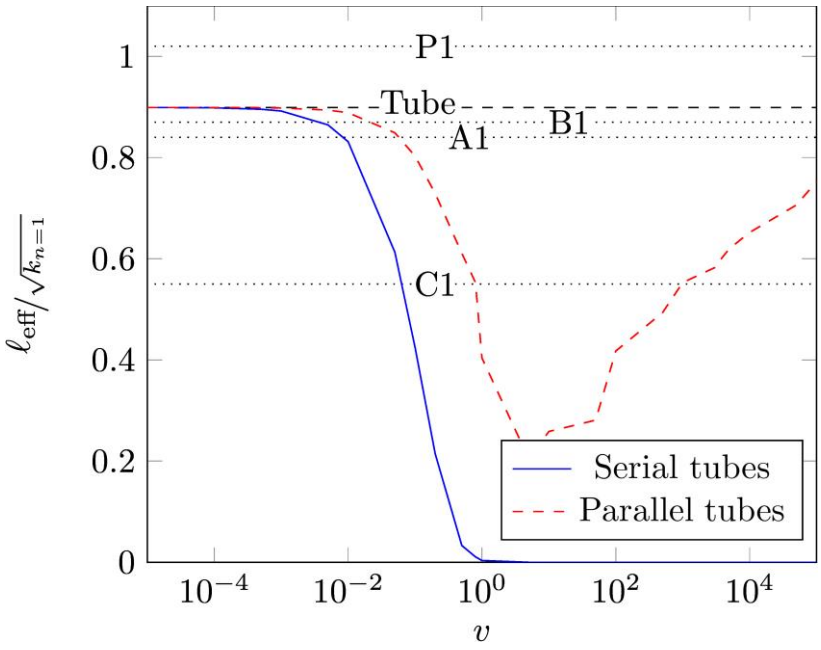

Figure 2 *Evolution of the dimensionless effective length with the variance of the bundle in parallel or serial, ($R_{mean} = 10\mu m$). The calculations are run for* $n = 0.7$. *The values for some of the porous media from [1] are also reported.*

A few important clarifications must be made at this point:

- We ran the calculations for a wide range of values of n (0.5 to 1.5) and the trend seems relatively independent of this parameter. Remarkably, despite the high complexity of the n dependency in the effective length expression, see Table 1, the choice of n does not significantly influence the critical velocity at which the transition occurs. This supports conclusions in [6], where the effective length was also found to be independent from this parameter.
- For better comparison with the results from [6], we add in Fig. 2 the values for the dimensionless effective length obtained in that paper for a Bentheimer sandstone, B1, a Clashach sandstone, C1, a packing of beads, P1, and a 2D cylinder array, A1. For all of them, $\sqrt{k_{n=1}}$ is a good order of magnitude estimation of the effective length (ℓ^*_{eff} is of order 1). Nonetheless we note that ℓ^*_{eff} is equal to 0.55 for medium C. In the framework of an order of magnitude approximation, the length $\sqrt{k_{n=1}}$ is however still a correct estimation.
- The ratio of maximal to minimal radii of the distribution is equal to 21 for $v = 10^{-1}$ and 2597 for $v = 1$. In the framework of this study, we choose to not investigate tubes bundles that have a variance above 10^{-1}. Although particular porous media present a very wide maximal to minimal pore size, e.g., carbonate media, we consider these latter as very specific. The pore space would be very complicated, and the model proposed by Zami-Pierre et al. [6] to predict the transition may not be applied in this case.

In summary, we observe that ℓ^*_{eff} is close to unity for all bundles (serial or parallel) up to a reasonable variance value (say $v = 10^{-1}$). By "close", we mean here that an order of magnitude approximation is correct. As explained in [6], the goal of the model is not to accurately predict the transition – which is a smooth phenomenon, definition-sensitive, pore structure dependent – but rather to estimate it. We may conclude that such artificial porous media give a transition between Newtonian and non-Newtonian regimes which can be reasonably estimated by Eq. 2.

Results show a different trend between the serial and parallel bundles. We observe in Fig. 2 that, as the serial bundle curve collapses to zero, the parallel one increases above a certain variance value. Modelling the effective length by $\sqrt{k_{n=1}}$ seems then to work better at high variances for the parallel bundle than for the serial one. To understand the curve behavior at high variance values, we calculate an approximation of the Newtonian permeability using the fact that the ratio of maximal to minimal radii is very large, so that we can simplify equations from Table 1.

Bundle in serial:
$$k_{n=1}^{v\gg1} = \frac{N^2 R_{min}^4}{8R_{max}^2} \tag{4}$$

Bundle in parallel:
$$k_{n=1}^{v\gg1} = \frac{R_{max}^2}{8} \tag{5}$$

Concerning the serial bundle, we clearly see that, for a large variance, the permeability becomes very sensitive to the smallest tube radius, Eq. 4. This was expected since all the fluid must go through this small section. On the other hand, the largest tube radius becomes the most important for the parallel bundle, as expected, Eq. 5. We can now adopt the same asymptotic approach for the effective length.

Bundle in serial:
$$\ell_{eff}^{v\gg1} = C(n)\frac{N\,R_{min}^3}{R_{max}^2} \simeq \sqrt{k_{n=1}^{v\gg1}}\frac{R_{min}}{R_{max}} \tag{6}$$

Bundle in parallel:
$$\ell_{eff}^{v\gg1} = C(n)R_{max} \simeq \sqrt{k_{n=1}^{v\gg1}} \tag{7}$$

Thanks to the formulation in Eq. 7, we can understand why the parallel bundle curve increases at high variance. Indeed, by increasing the variance the parallel bundle will contain a very large and dominant tube, and the apparent behavior will then be close to a single tube case with this maximal radius. On the other hand, the expression $\ell_{eff}^{v\gg1}$ for the serial bundle tends to zero with increasing variance, i.e., increasing maximal radius. The use of $\sqrt{k_{n=1}}$ as effective length in such cases becomes completely irrelevant.

Model comparison with experiments

In addition to conceptual tubes bundles, we can also test the robustness of the model with regard to experimental datasets provided by the literature. As described earlier, a common methodology used in core-flood experiments consists in calculating an apparent shear rate, $\dot{\gamma}_{app}$ as in Eq. 8. The fitting parameter α is tuned such as at the transition, $\dot{\gamma}_{app} = \dot{\gamma}_c$.

$$\dot{\gamma}_{app} = \alpha\frac{4\langle U\rangle_{FL}}{\sqrt{8\,k_{n=1}/\phi}} \Longrightarrow \langle U_c\rangle_{FL} = \frac{1}{\sqrt{2\phi}\alpha}\,\dot{\gamma}_c\sqrt{k_{n=1}}. \tag{8}$$

Instead of dealing with such an apparent quantity, the model presented by Zami-Pierre et al. [6] directly predicts the critical intrinsic average velocity, Eq. 2. A comparison can be done between these two approaches, through Eq. 8. The apparent shear rate approach is actually similar to the proposed model. A prefactor – equal to $1/\sqrt{2\phi}\alpha$ – is simply added to the original formulation.

We looked for core-flood experiments that used a non-Newtonian fluid (Xanthan) [14,16,21] and where the parameters used in the apparent shear rate formulation were detailed. We reported the values of the associated prefactor for several references and porous media in Table 2.

Reference	Porous medium	α	ϕ	$1/\sqrt{2\phi}\alpha$
J. Lecourtier et al. [14]	Beads packing	1.7	0.48	0.60
G. Chauveteau [21]	Beads packing	1.4	0.41	0.79
G. Chauveteau [21]	Sandstone	4.5	0.09	0.53
G. Chauveteau [21]	Carborunbum	1.1	0.46	0.95
A. Fletcher et al. [16]	Clashach	4.48	0.14	0.41
A. Fletcher et al. [16]	Berea	6.0	0.20	0.26

Table 2 *Calculated prefactor* $1/\sqrt{2\phi}\alpha$ *for several core-flood experiments for polymer solutions through different type of porous media.*

From Table 2, we observe that, for different porous media, the prefactor value is compatible with the estimate for the critical transition velocity. In other words, and this has an important practical significance, the "traditional" representation of the transition seems to introduce an artificial dependence with the porosity which is not supported by the physics of the flow for all type of media. As a consequence, this latest crtierion needs to introduce a correcting factor which may vary strongly with the nature of the porous medium. In the new approach, the proposed criterion is more robust and likely to suppress an unnecessary parameter.

We also observe that the prefactor value is always smaller than 1. We recall that, the model from Zami-Pierre et al. [6] is based on a simple rheology only. In an actual core-flood, many physical phenomena may occur (e.g., rearrangement of polymer chains, wall interaction, degradation…) which are not taken into account in the proposed model. It seems like, from a macro-scale point of view, the sum of these phenomena trigger the transition sooner.

Flow patterns

Among the results obtained in [6], one of them is that the nonlinearity induced by the rheology has a weak impact on the evolution of the flow field properties for PLCO fluids. In particular, the probability density function of the velocity field normalized by the average velocity remains relatively unchanged by the non-Newtonian behavior. This is remarkable since we could expect the nonlinearity to drastically change the flow field. For instance, dealing with a shear-thinning fluid, we might think that when the fluid in a pore-throat becomes non-Newtonian, the viscosity will start to drop, reducing the energy loss through this pore-throat. As a result the velocity would increase in this pore-throat and the flow field would be drastically modified. Such feed-back being not observed, we explore this interesting and somehow intriguing result by studying the dissipative energy lost by viscous friction per unit volume, $\varepsilon = \mu\dot{\gamma}^2$.

For the four porous media in [6] presented earlier, we first define a dimensionless dissipative energy by $\varepsilon^* = \varepsilon/\varepsilon_{max}$. This definition allows us to work with a field variable between 0 and 1. We note ε_0^* the dissipative energy field of a Newtonian fluid. As long as the flow velocity is too low to exhibit non-Newtonian phenomena ($\langle U\rangle_{FL} \ll \langle U_c\rangle_{FL}$), the field ε^* does not change and is equal to ε_0^*. When the flow velocity starts to be high enough ($\langle U\rangle_{FL} = O(\langle U_c\rangle_{FL})$), the field ε^* should slightly deviate from ε_0^*. To quantity this deviation, we define an auto-correlation function F for the dissipative energy as,

$$F_{\varepsilon^*\varepsilon_0^*}(U^*) = \frac{\langle \varepsilon^*\varepsilon_0^*\rangle}{\langle \varepsilon_0^*\varepsilon_0^*\rangle}, \tag{9}$$

with $U^* = \langle U\rangle_{FL}\,/\langle U_c\rangle_{FL}$. With this definition, when the flow regime is fully Newtonian ($U^* \ll 1$), the auto-correlation function is equal to 1, i.e., ε^* and ε_0^* are equal. As the velocity increases, the flow field starts to exhibit deviations from the Newtonian pattern. To prove that the flow patterns seem to remain statistically unchanged when the fluid undergoes nonlinear behavior induced by non-

Newtonian effects, we could have studied other variables than the dissipative energy, e.g., shear rate, velocity magnitude or kinetic energy. However, the dissipative energy is very interesting since it is involved in the permeability and points at the region where the fluid firstly displays non-Newtonian effects [6]. Fig. 3 shows the function F versus the dimensionless velocity U^* for the porous media from [6] as well as a converging tube ($\alpha = R_{outlet}/R_{inlet} = 0.6$) and a simple tube ($\alpha = 1.0$).

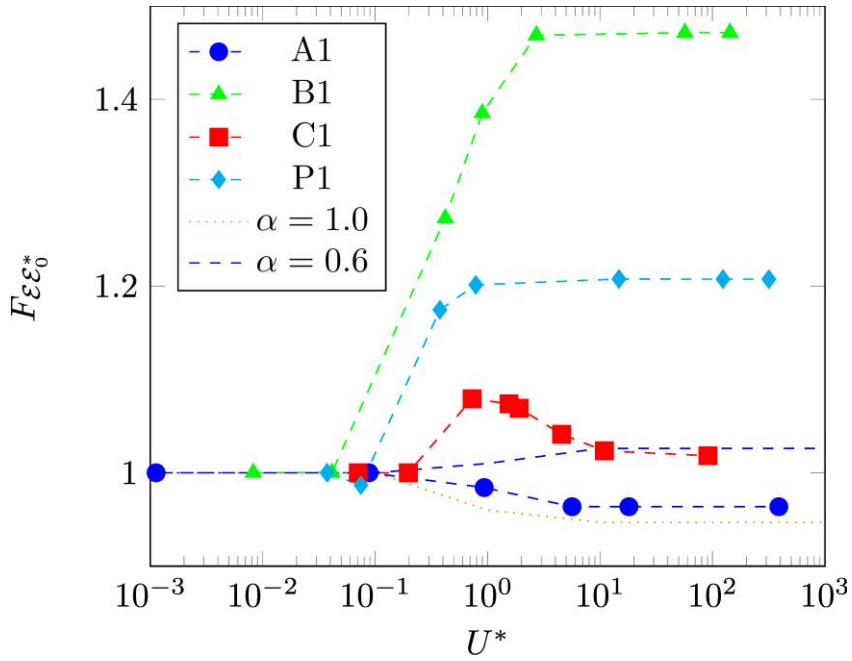

Figure 3 *Evolution of F versus the dimensionless average velocity U^*. Porous media investigated: A1, B1, C1 and P1 from [6], as well as a converging tube ($\alpha = 0.6$) and a simple tube ($\alpha = 1.0$). Rheology: $n = 0.75$ & $\dot{\gamma}_c = 1s^{-1}$.*

Fig. 3 shows the existence of a plateau obtained at high flow velocity for all investigated porous media. We denote the plateau value as $F_{U^* \gg 1}$. We could have expected that the function F continues to increase with U^*, the flow field being less and less correlated to the Newtonian flow field. However, the plateau clearly indicates that, despite the flow complexity induced by the fluid nonlinearity, the dissipative energy fields remain correlated to the Newtonian field. We also notice that the plateau value is different for all media. Since the rheology is fixed for the cases in Fig. 3, this means that $F_{U^* \gg 1}$ is an intrinsic trace of the topology/rheology interaction, or, in other words, an intrinsic property of the considered medium.

Further insight can be gained by looking at simple analytical solutions for tubes. We can calculate $F_{U^* \gg 1}$ for a tube or a converging tube, see Fig. 2. In the case of a tube, $F_{U^* \gg 1}$ simply depends on n and is equal to $6n/(5n+1)$. This case is very distinct from the others since the effect of the topology is non-existent and the deviation of $F_{U^* \gg 1}$ from 1 is purely due to the rheology. Concerning the converging geometry ($\alpha = 0.6$), the value of $F_{U^* \gg 1}$ is different. Turning to real porous media, where pore throats may be assimilated to converging-diverging tubes, this suggests that the pore size distribution (PSD) may affect directly the plateau value. When the PSD is wide, the inherent porous medium topology would be more likely to play a role in $F_{U^* \gg 1}$.

This idea might help in the analysis of results from Fig. 3. The PSD is wider for sandstone media B1 & C1, than for the beads packing P1, which itself has a wider PSD than medium A1 [6]. The classification based on $F_{U^* \gg 1}$ works for samples B, P & A, but not for medium C, which has a plateau close to unity. We hypothesise that medium C is so particular that it could actually be very well seen as a series of single tubes. Indeed, although its PSD is wide, only a few pore-throats are actually be solicited by the flow. A crucial distinction emerges here between the PSD and the actual solicited pores. Further work is needed to confirm this theory.

Conclusions

In this paper we have tested the robustness of the macro-scale transition model of a non-Newtonian fluid flowing through porous media proposed by Zami-Pierre et al. [6]. The tests were performed by comparing the model with results obtained for conceptual bundles of tubes and actual core-flood experiments. We found that the model is robust and that the square root of the Newtonian permeability provides a good estimation of the characteristic length-scale defining the non-Newtonian transition. A comparison with traditional transition criteria suggests that the introduction of the porosity in the criteria might be not pertinent. We also studied the relative stability of the flow patterns when the fluid changes to non-Newtonian behavior. In agreement with [6], we found that the normalized flow statistics remain unchanged by studying correlation functions for the viscous dissipative energy field. Further work is needed to quantify the influence of the topology and the rheology on the flow statistics.

Acknowledgments

We thank Total for the support of this work. This work was granted access to the HPC resources of CALMIP supercomputing center under the allocation 2015-11.

References

[1] J.V. Soulis et al, Non-Newtonian models for molecular viscosity and wall shear stress in a 3D reconstructed human left coronary artery. Medical engineering & physics, 9-19 (2008)
[2] S. Advani, Flow and Rheology in Polymer Composites Manufacturing, Elsevier (1994)
[3] L.W. Lake, Fundamentals of enhanced oil recovery. Society of Petroleum Engineers (1986)
[4] W. Cannella et al, Prediction of xanthan rheology in porous media. SPE Annual Technical Conference and Exhibition (1998)
[5] R.S. Seright et al, New insights into polymer rheology in porous media. SPE Journal, 35-42 (2011)
[6] Zami-Pierre et al, Transition in the flow of power-law fluids through isotropic porous media. Physical Review Letters, *Accepted for publication in Physical Review Letters* (2016)
[7] O. Gipouloux et al, Computation of the filtration laws through porous media for a non-Newtonian fluid obeying the power law. Computational Geosciences, 127-153 (1997)
[8] D. Getachew et al, Macroscopic Equations of Non-Newtonian Fluid Flow and Heat Transfer. Journal of Porous Media, 273-283 (1998)
[9] S. Liu et al, On non-Newtonian fluid flow in ducts and porous media. Chemical Engineering Science, 1175-1201 (1998)
[10] G. Chauveteau et al, Concentration Dependence of the effective Viscosity of Polymer Solutions in Small Pores with Repulsive or Attractive Walls. Journal of Colloid and Interface Science, 41-54 (1984)
[11] T. Chevalier et al, Darcy's law for yield stress fluid flowing through a porous medium. Journal of Non-Newtonian Fluid Mechanics, 57-66 (2013)
[12] M. Vakilha et al, Modelling of power-law fluid flow through porous media using smoothed particle hydrodynamics. Transport in Porous Media, 331-346 (2008)
[13] J. Bleyer et al, Breakage of non-Newtonian character in flow through a porous medium: Evidence from numerical simulation. Physical Review E, 89 (2014)
[14] J. Lecourtier et al, Xanthan fractionation by surface exclusion chromatography. Macromolecules, 1340-1343. (1984)
[15] K.S. Sorbie et al, Rheological and transport effects in the flow of low-concentration xanthan solution through porous media. Journal of Colloid and Interface Science, 74-89 (1991)
[16] A. Fletcher et al, Measurements of polysaccharide polymer properties in porous media. SPE International Symposium on Oilfield Chemistry (1991)
[17] R. B. Bird et al, Transport Phenomena, Wiley (1960)

[18] R. H. Christopher, Power-law flow through a packed tube, Industrial & Engineering Chemistry Fundamentals, 4, 422-426 (1965)
[19] J. G. Savins, Non-Newtonian Flow through Porous Media, Ind. and Eng. Chem, 61 18-47 (1969)
[20] UTCHEM, Technical Documentation (2011)
[21] G. Chauveteau, Rodlike polymer solution flow through fine pores: influence of pore size on rheological behavior, Journal of Rheology, 26, 111-142 (1982)